

# Digital control of tunneling accelerometer

Chris Burgner\*, Zi Yie\*, Nitin Kataria†, Laura Oropeza\*, Karl Åström\*, Forrest Brewer† and Kimberly Turner\*

\*Mechanical Engineering

†Electrical and Computer Engineering

University of California at Santa Barbara

Santa Barbara, California 93117

Email: cburgner@umail.ucsb.edu

**Abstract**—A controller for a tunneling accelerometer has two tasks: to establish tunneling and to maintain tunneling during acceleration. This paper describes the design and implementation of a digital controller that accomplishes these tasks and provides the appropriate gain switching. The control law is based on a standard configuration of an observer and state feedback. A digital controller is implemented because the controller parameters can be easily adjusted, thereby allowing for rapid prototyping. The design methodology presented here can be used as a general plug-and-play controller platform for a range of MEMS sensors. The performance of the digital controller is illustrated experimentally using metrics such as tracking response, drift, noise floor and response linearity.

## I. INTRODUCTION

The measurement of acceleration is a fundamental element in inertial guidance and continues to have a wide application in both military and consumer products. Tunneling is a phenomena which occurs when electrons jump between a pair of electrodes separated by a gap on the order of  $1nm$ . Tunneling has been exploited as a highly sensitive method for measuring position and is well established commercially in scanning tunneling microscopes.

Micromachined accelerometers have been built on a variety of principles such as capacitive, piezoresistive and piezoelectric [1]. Tunneling is extremely sensitive due to its exponential dependence on displacement. As well, the tunneling current is invariant to temperature changes. These features make tunneling accelerometers highly attractive. A tunneling accelerometer usually has four key components: a proof mass, support springs, an actuator and a tunneling tip. The accelerometer works by employing force feedback from a controller. When an external acceleration is applied on the accelerometer, an inertial force is experienced on the proof mass which causes a displacement and compresses the springs. The displacement is then sensed through the tunneling current via the tunneling tip. In response, the controller generates a signal that will allow the actuator to produce a force to cancel out the inertial force. Thus, the proof mass is held in a constant position and only moves in a small zone. The generated feedback force is measured, which is proportional to the applied external acceleration.

Considerable work has been done on the control of tunneling accelerometers in the past, but most have complicated designs and analog implementation [2], [3], [4]. This work develops a methodology for the control design, as well as

the software and hardware for prototyping feedback systems for digital control of MEMS sensors. Digital controllers are desirable because they can be tailored through flexible code and improved upon without the redesign of hardware.

Tunneling accelerometers have a particular problem in that the controller must blindly close the tip gap to a point where tunneling starts. In our case, this is from approximately  $1000nm$  to about  $1nm$ . The controller must react quickly in order to avoid crashing the tip. The flexibility of digital control overcomes this problem by using gain switching, which not only safely guides the tip, but also acts to maintain the necessary tunneling current and keep fluctuations in the tip gap small.

## II. ACCELEROMETER MODEL

Our tunneling accelerometer, seen in Figure 1, is based on the design in [4] and fabricated using a standard SOI process.

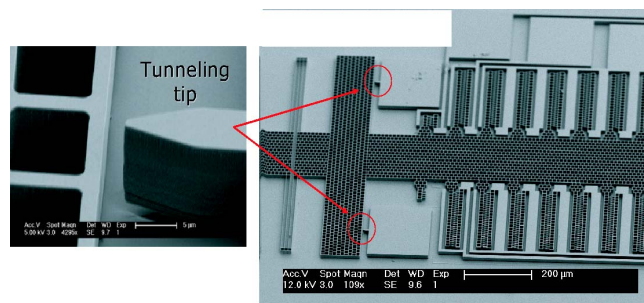


Fig. 1. SEM picture of the device ( $20 \mu mSi/5 \mu mSiO_2$ ) and a close up view of the tunneling tip.

In order for tunneling to occur, a metal coating is applied over the the tunneling electrodes. A layer of Au is chosen to be the electrode metal, a layer of Ti acts as a metal adhesion layer on the silicon, and a layer of Pt acts as a diffusion boundary between the Ti and Au to keep the Ti from reaching the gold surface which would inhibit tunneling [7]. Theoretically, the tunneling current is given by:

$$I_t \propto V_b \exp(-\alpha\sqrt{\phi}x_0)$$

where  $x_0$  is the gap between tunneling electrodes,  $V_b$  is the bias voltage applied across the electrodes,  $\alpha$  is the tunneling constant, and  $\phi$  is the energy work function.

The accelerometer can be simplified to a standard mass-damper-spring model whose equation of motion is given by:

$$m \frac{d^2x}{dt^2} + c \frac{dx}{dt} + kx = F_e + mw$$

where  $m$  is the mass,  $c$  is the damping coefficient,  $k$  is the spring stiffness,  $w$  is the external acceleration, and  $F_e$  is the electrostatic force generated by the combdrive. Fringing fields are ignored in the combdrive actuator and a parallel plate assumption is made such that the electrostatic force is governed by:

$$F_e = N \frac{h\epsilon}{d} V^2$$

where  $N$  is the number of comb fingers,  $d$  is the gap between the fingers,  $h$  is their height,  $\epsilon$  is the dielectric constant in air, and  $V$  is the applied voltage.

By linearizing the equations [5], our accelerometer model becomes:

$$\begin{aligned} \text{Combdrive actuator:} & F_e = k_a u \\ \text{Mass-damper-spring:} & m\ddot{x} + c\dot{x} + kx = F_e + mw + n_{th} \\ \text{Tunneling current:} & I_t = k_t x + n_t \\ \text{Preamplifier:} & y = k_v (RI_t + n_R) \end{aligned}$$

The combdrive actuator model is static and  $k_a$  is the linearized actuator gain which depends on the nominal voltage. The mass-damper-spring equation is used to describe the position of the mass. The tunneling current is linearized about the nominal tunneling distance of  $1nm$  with  $k_t$  representing the linearized tunneling gain. The preamplifier converts the current into a voltage signal. It has two stages, but for simplicity, much of the dynamics are neglected. The first stage has an effective feedback resistance of  $R$ , and the second stage has a voltage gain of  $k_v$ . The noise sources are represented by thermal noise  $n_{th}$ , tunneling noise  $n_t$ , and resistor noise  $n_R$ . The noises are obtained from physics and their characteristics have been studied in [5]. Some numerical parameter values for our model are summarized in Table I.

TABLE I  
SYSTEM PARAMETERS

Mass	$m$	4.917 $\mu\text{g}$
Resonant frequency	$f_0$	4.2 kHz
$Q$ -value	$Q$	10
Actuator gain	$k_a$	$9.2 \times 10^{-7} \text{N/V}$
Tunneling gain	$k_t$	4 A/m
Preamplifier resistance	$R$	10.2 M $\Omega$
Preamplifier voltage gain	$k_v$	2

### III. CONTROL DESIGN AND IMPLEMENTATION

Details of the control design are given in [6]. Briefly, we assume a linear system described by:

$$\dot{x} = Ax + B(u + w) \quad y = Cx$$

where  $x$  is the state variable,  $w$  is the external acceleration that we want to measure,  $u$  is the control signal, and  $y$  is the error signal that we try to keep small. In this model we have also assumed that the control signal enters at the same place as the acceleration.

A simple model for the dynamics of the external acceleration is to assume that it is constant but unknown, hence:

$$\frac{dw}{dt} = 0$$

The control law is relatively straight forward and based on a standard configuration of an observer and state feedback. Thus, it can be stated as follows:

$$\begin{aligned} \dot{\hat{x}} &= A\hat{x} + B(u + \hat{w}) + \begin{bmatrix} l_1 \\ l_2 \end{bmatrix} (y - C\hat{x}) \\ \dot{\hat{w}} &= l(y - C\hat{x}) \\ u &= -\hat{w} + [k_1 \quad k_2] \hat{x} \end{aligned}$$

where  $\hat{x}$  and  $\hat{w}$  are the estimated state and acceleration, respectively, while  $l_1$ ,  $l_2$ ,  $l$  are the observer gains and  $k_1$ ,  $k_2$  are the feedback gains.

With one state being the unknown acceleration  $w$ , the other states are the position and the velocity of the mass. The system matrices become:

$$\begin{aligned} A &= \begin{bmatrix} 0 & 1 \\ -k/m & -c/m \end{bmatrix} & B &= \begin{bmatrix} 0 \\ 1 \end{bmatrix} \\ C &= [k_s \quad 0] \end{aligned}$$

where  $k_s = k_v k_t R$  and the control signal is scaled with  $m/k_a$ .

The resulting controller is of third-order and illustrated by the block diagram shown in Figure 2. The controller can be interpreted as an integrator in cascade with a second-order notch filter. The notch filter attenuates the resonant mode of the mass. The feedback gains  $k_1$  and  $k_2$  determine how well the mass is kept to its center position.

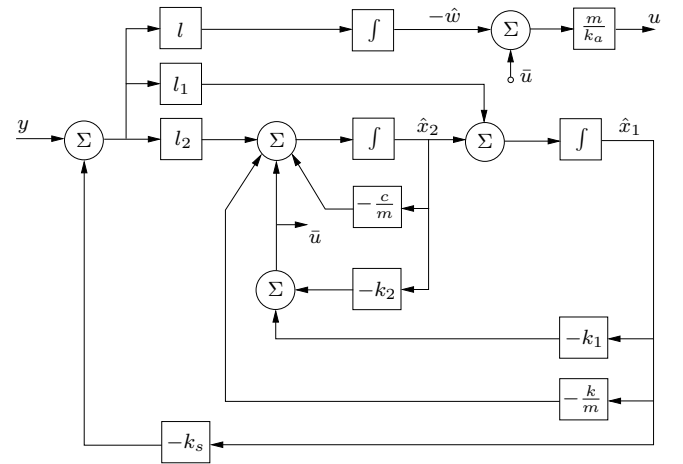


Fig. 2. Block diagram of the controller.

The controller was implemented on a National Instruments CompactRIO platform, which contains a field-programmable

gate array (FPGA) and programmed through the LabVIEW software environment. For numerical reasons, a scaled version of the controller was implemented to give a balanced representation of the matrices. In operation, the output voltage from the preamplifier was sampled by the controller, running on the CompactRIO, to generate the appropriate control action.

#### IV. EXPERIMENTAL RESULTS

To test the system, it was placed on a rate table with computer controlled velocity and acceleration. Figure 3 shows the experimental set up. The CompactRIO was also placed on the rate table and the signals were transferred to the computer via a wireless router. The picture shows the preamplifier box on the left and the compactRIO with the router on the right. The preamplifier was built on a printed circuit board using ultra-low noise op-amps and operated with batteries. The accelerometer was mounted directly onto the printed circuit board itself.

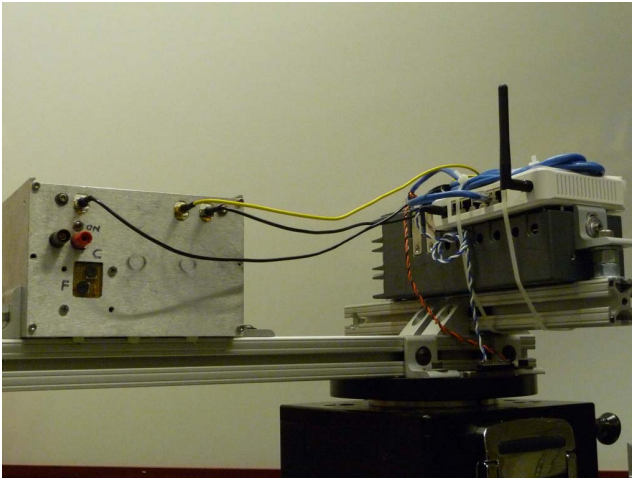


Fig. 3. Experimental set-up showing device (inside the box), CompactRIO, and associated hardware all mounted on a rate table. Signals are transmitted wirelessly through the router from the CompactRIO to a host PC which is used to store and display the real-time data.

The gain of the preamplifier was chosen to correspond to a  $20mV$  of DC output for a nanoampere of tunneling current. The output of the preamplifier was sampled by the controller running on the CompactRIO at a sampling frequency of  $62.5kHz$  which is limited by calculation time required on the FPGA, bandwidth of the control loop, and the preamplifier roll-off. In Figure 4 we observe the two stages of controller operation. First the controller ramps up its control voltage linearly as the proof mass blindly approaches the tunneling tip. At this point the only measured signals are due to the resistor noise. Second, tunneling is onset near a distance of  $10\text{\AA}$  and at approximately 50sec, the controller is switched to a higher gain making it faster such that tunneling is locked at a reference voltage of  $40mV$ .

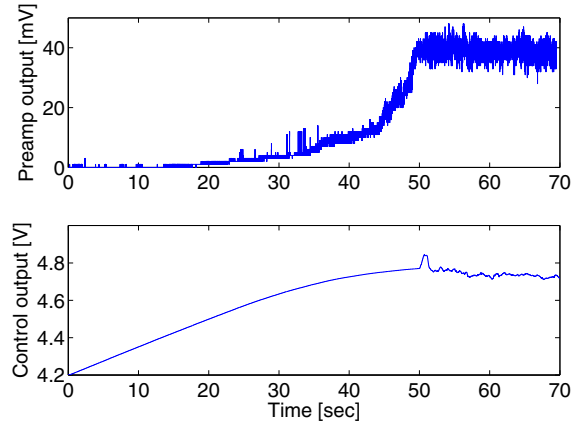


Fig. 4. The controller signal and preamplifier output during tunneling approach and lock-in. Notice the characteristic exponential rise in tunneling current as the mass approaches the tunneling tip.

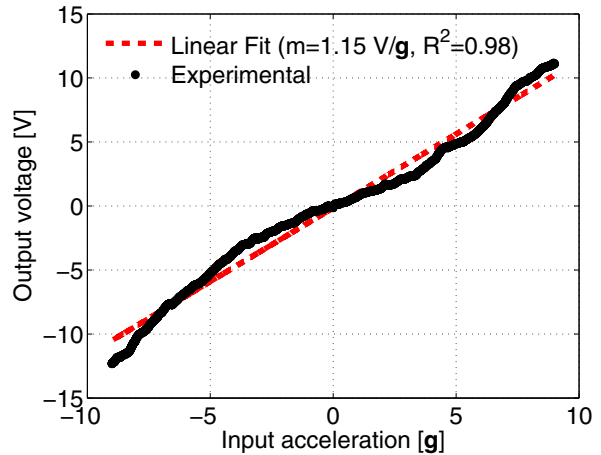


Fig. 5. Controller output response (solid) to a ramp input of  $\pm 9g$ . The ramp response was obtained by placing the accelerometer off the central axis of a rate table. The angular velocity supplied by the rate table applied a centripetal acceleration which was measured by the accelerometer.

An acceleration ramp input over the range of  $\pm 9g$  was applied to the device and the response is observed in Figure 5. Device sensitivity is calculated analytically described in [8] to be  $1.2V/g$  which is very near the experimental result of  $1.15V/g$ . Square of the correlation coefficient is  $0.98$  indicating a good linear response in the dynamic range of  $\pm 9g$ . Misalignment of the device along the centripetal axis would cause the device to sense the angular acceleration in the normal direction which may explain the symmetric error seen in Figure 5.

The drift of the device was recorded over a period of one hour. After an initial rise, the device output reaches a plateau

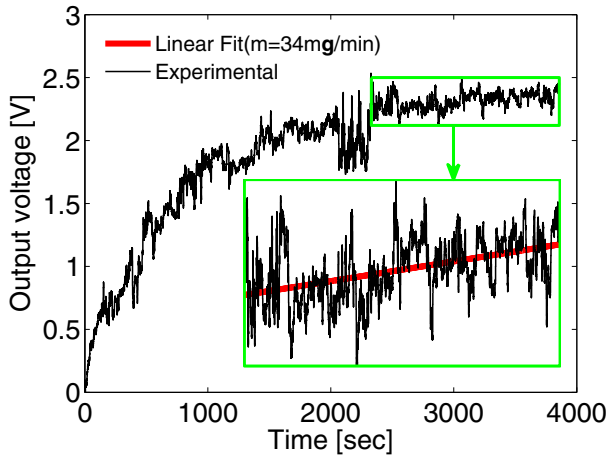


Fig. 6. Controller output over a period of 1 hr. Accelerometer maintains tunneling over the entire period and drift is calculated to be 34mg/min.

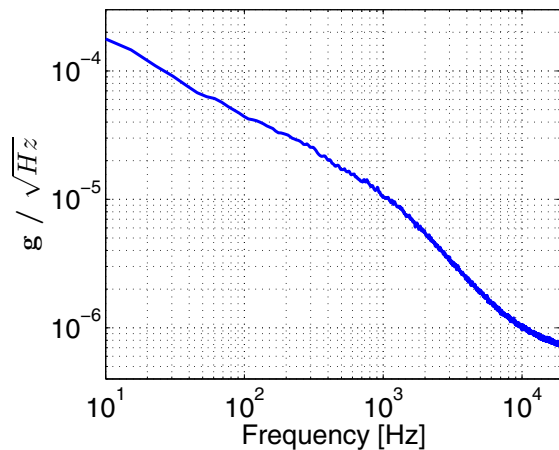


Fig. 7. Noise spectrum of the tunneling accelerometer. Noise is dominated by  $1/f$  up to 1kHz and then  $1/f$  squared until it flattens out near 10kHz at  $1\mu\text{g}/\sqrt{\text{Hz}}$ .

where the drift is calculated to be 34mg/min as illustrated in Figure 6.

The noise spectrum of the preamp output is plotted in Figure 7. At low frequencies the noise is dominated by  $1/f$  which may be explained in [9] as a surface adsorption-desorption process. The noise floor is seen to be less than  $1\mu\text{g}$  past 10kHz which is ultimately set by the mechanical thermal noise [5], [10].

## V. CONCLUSION

A methodology for control design, software and hardware for prototyping feedback systems for digital control of MEMS

sensors is presented. The controller implementation is carried out on an FPGA using a LabView CompactRIO interface. Control is applied to a tunneling accelerometer, similar in design as [4], which is a particularly difficult device to control due to the two necessary stages of control the strict tip displacement fluctuations to avoid crashing. The digital controller is verified through experiment which shows the effectiveness of gain switching to achieve both approach and tunneling lock. Device metrics obtained using digital control are superior to those in [4] which implemented analog.

Control is based on the linear analysis of the accelerometer model. Because nonlinearities exist in the combdrive actuators and the tunneling current, compensation for these effects can be introduced due to the flexibility of digital control. The actuator nonlinearity can be compensated for by passing the actuation voltage through a square root function and the exponential characteristic of the tunneling current can be compensated for by a passing the the current through a logarithmic.

## ACKNOWLEDGMENT

The authors would like to thank Jeannie Falcon, Javier Gutierrez, and Brian MacCleery at National Instruments for their valuable support on LabVIEW and the CompactRIO platform.

## REFERENCES

- [1] N. Yazdi, F. Ayazi, and K. Najafi, "Micromachined inertial sensors," *Proceedings of the IEEE*, vol. 86, pp. 1640-1659, August 1998.
- [2] C.H Liu, H. Rockstad and T. Kenny, "Robust controller design via  $\mu$ -synthesis for high-performance micromachined tunneling accelerometers," *Proceedings of the American Control Conference*, San Diego, CA, 1999.
- [3] A. Partridge, J. Reynolds, J. Grade, B. Kane, N. Malnuf, G. Kovacs, T. Kenny, "An integrated controller for tunnel sensors." *IEEE Journal of Solid-State Circuits*, vol. 34, pp. 1099-1107, 1999.
- [4] P.G Hartwell, F. Bertsch, S. Miller, K. Turner and N. MacDonald, "Single mask lateral tunneling accelerometer." *Micro Electro Mechanical Systems, 1998. Proceedings., The 11th annual International workshop on*, pp. 340-344, 25-29 Jan 1998.
- [5] L. Oropeza-Ramos, N. Kataria, K. Åström, F. Brewer and K. Turner, "Noise analysis of a tunneling accelerometer based on state space stochastic theory," *In Solid-State Sensor, Actuator, and Microsystems Workshop*, Hilton Head, SC, 2008.
- [6] Z. Yie, N. Kataria, C. Burgner, K. Åström, F. Brewer and K. Turner, "Control design for force balance sensors," *Proceedings of the American Control Conference*, St. Louis, MO, 2009.
- [7] T. Kenny, W. Kaiser, H. Rockstad, J. Reynolds, J. Podosek and E. Vote, "Wide-bandwidth electromechanical actuators for tunneling displacement transducers," *Journal of Micromelectromechanical Systems*, vol. 3 Issue 3, pp 97-104, September 1994.
- [8] N. Yazdi et al. "Micromachined inertial sensors." *Proceedinigs of the IEEE*, vol. 86, pp. 1640-1659, August 1998.
- [9] J. Wang, P. Zavracky, N. McGruer and R. Morrison, "Study of tunneling noise using surface micromachined tunneling tip devices," *Transducers 97*, vol 1, pp 467-470, June 1997
- [10] T. Gabrielson, "Mechanical-thermal noise in micromachined acoustic and vibration sensors," *IEEE transactions on Electron Devices*, vol. 40, pp. 903-909, May 1993.